Theor Chem Acc (2010) 127:661–669
DOI 10.1007/s00214-010-0772-0

REGULAR ARTICLE

Computational study on the energies and structures of the [H, Si, N, C, S] isomers

Simon R. T. Neil · Corey J. Evans

Received: 24 May 2010 / Accepted: 24 May 2010 / Published online: 11 June 2010

Abstract Computational chemistry methods have been used to study the lowest lying [H, Si, N, C, S] isomers which are of astrochemical interest. A number of [H, Si, N, C, S] isomers have been investigated at the B3LYP/aug-cc-pVTZ level of theory. Of these, the seven lowest isomers have been further investigated using different levels of theory, including MP2 and QCISD(T). It has been found that at all levels of theory the lowest energy isomer is HSi(S)CN. For the seven lowest isomers, rotational constants and vibrational frequencies have been evaluated. In addition, the enthalpies of formation of the seven lowest isomers have been evaluated using the G3MP2 multilevel method and shows that the isomers are relatively thermodynamically stable compared to other silicon-containing species that have been detected in space. The structures and energies of the lowest lying excited singlet states of these isomers have also been investigated. For the isomers HSi(S)CN, HSi(S)NC, HS–SiCN and HS-SiNC, the lowest lying excited state is predicted to be non-planar, while for HSiNCS the lowest lying excited state is predicted to be planar with similar structural changes occurring on excitation as seen in HSiNCO and HSiNC.

Keywords Ab initio · Optimized structure · Vibrational frequency · Isomerisation · Enthalpies of formation · Sulphur-containing compounds · Silicon-containing compounds · Astrochemistry · Electronic spectroscopy · Microwave spectroscopy · Computational chemistry

1 Introduction

Recently, our group has looked at a number of silicon-containing species with the aim of finding new molecules that have a strong potential of being found in space. In our previous study, we carried out work on the [H, Si, N, C, O] isomers using ab initio techniques and found that lowest lying isomer is HSi(O)CN (at the MP2/aug-cc-pVTZ level of theory) [1]. From this work, we went onto observe the previously unknown species HSiNCO using laser-induced fluorescence and determined the rotational and centrifugal distortion constants of both its $\tilde{X}^1A'$and $\tilde{A}^1A''$ electronic states [2]. We have also carried out a laser spectroscopic study on the $\tilde{X}^1A'$ and $\tilde{A}^1A''$ electronic states of HSiNC, which has previously been detected using microwave spectroscopy and is thought to be an excellent candidate for detection in space [3].

To further our work on organosilicon compounds, this paper aims at examining the possible isomers of [H, Si, N, C, S]. Sulphur has a cosmic abundance which is only slightly less than silicon, and therefore it is feasible that some of the [H, Si, N, C, S] isomers studied in this work will be present in the environs of space. There are presently about 15 sulphur-containing molecules, including SiS, that have been detected in space [4]. Therefore, it is hoped this work will aid in the detection of some of the [H, Si, N, C, S] isomers in both the laboratory and in space.

Electronic supplementary material The online version of this article (doi:10.1007/s00214-010-0772-0) contains supplementary material, which is available to authorized users.

S. R. T. Neil · C. J. Evans (✉)
Department of Chemistry, University of Leicester,
University Road, Leicester LE1 7RH, UK
e-mail: cje8@le.ac.uk

Present Address:
S. R. T. Neil
Department of Chemistry, Physical and Theoretical Chemistry
Laboratory, University of Oxford, South Parks Road,
Oxford, OX1 3QZ, UK

2 Theoretical methods

For the most part, calculations were carried out using the Gaussian03 (G03) suite of programs [5]. The geometries of the different species and their isomers were fully optimized at different levels of theory using the augmented double and triple zeta correlated consistent basis set (aug-cc-pVDZ/aug-cc-pVTZ) of Dunning et al. [6, 7]. The methods used include the hybrid density functional method B3LYP, the second-order Møller-Plesset method (MP2) and the quadratic configuration interaction method including singles and doubles, QCISD [8, 9]. Further single-point calculations were carried out using QCISD(T), with the isomers fixed to their QCISD-optimized geometries. For all geometry optimizations, a tight convergence criterion was used, while for B3LYP calculations an ultrafine grid was employed. For accurate relative energies and evaluation of thermodynamic properties, the G3B3 and G3MP2 methods, as implemented in G03, were used. Vibrational frequencies were calculated at the different levels of theory to check if the optimized structures were true minima. The MP2 and QCISD calculations were carried out using the standard frozen core method. For the planar molecules, the geometry optimizations were carried out with symmetry constraints, while for non-planar systems no symmetry constraints were used. Multiconfiguration SCF (MC-SCF) calculations were carried out as implemented in the MOLPRO suite of programs using the aug-cc-pVTZ basis set with (13, 2) closed and (10, 4) active orbitals [10]. CIS and SAC-CI calculations, as implemented in G03, were carried out on a number of isomers to determine excited state structures and transition energies [11]. Natural bond orbital analysis (NBOA) was carried out using NBO version 3.1 (as implemented in G03) and were evaluated using the B3LYP-optimized geometries [12]. Calculations were run on several computer clusters including the system managed by EPSRC National Service for Computational Chemistry Software in addition to the University of Leicester Mathematical Modelling Centre's supercomputer which was purchased through the HEFCE Science Research Investment Fund. The visualization software GaussView and MOLDEN were used throughout this work [13, 14].

3 Results and discussion

A series of computational chemistry calculations were carried out on a number of different isomeric forms of [H, Si, N, C, S]. The optimized geometries and vibrational frequencies of 22 different isomers were calculated at the B3LYP level of theory (see the supplementary data for information about the energies of all 22 isomers). Figure 1 shows the seven lowest [H, Si, N, C, S] isomers in the $\tilde{X}^1A'$ electronic state using the B3LYP/aug-cc-pVTZ level of theory. In all cases, the electronic configuration of the singlet species is $18\,a'^2\,4a''^2$. As can be seen from Fig. 1, the seven lowest isomers (S1-S7) are all within approximately 46 kJ/mol of each other. At the B3LYP/aug-cc-pVTZ level of theory, the lowest isomer (S1) was found to be HSi(S)CN, which is the sulphur analogue of formyl cyanide, while the isocyanide analogue, HSi(S)NC, is only 5.0 kJ/mol higher in energy. This is different from that found from the study on the [H, Si, N, C, O] isomers, where *cis*-HOSiCN or *cis*-HOSiNC (theory dependent) were the lowest lying isomers [1]. Isomers S3 and S4 are the *trans* forms of HSSiCN and HSSiNC and are situated 18.0 and 21.3 kJ/mol higher in energy. The next two isomers are *cis*-HSSiCN and *cis*-HSSiNC, these are estimated to be 25.5 and 28.0 kJ/mol higher in energy than the lowest lying isomer. The next highest isomer is the sulphur analogue of HSiNCO, HSiNCS, and is predicted to be 43.9 kJ/mol higher in energy.

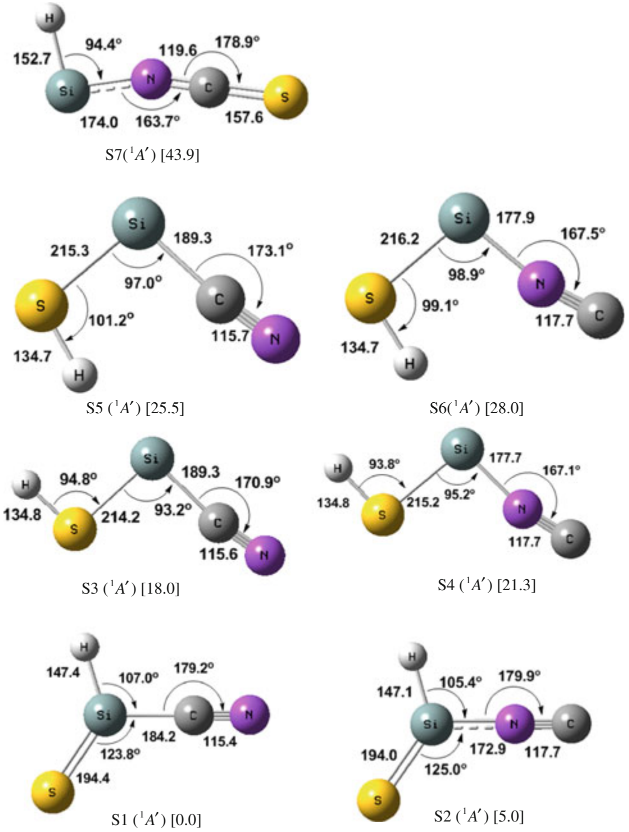

S7($^1A'$) [43.9]

S5 ($^1A'$) [25.5]

S6($^1A'$) [28.0]

S3 ($^1A'$) [18.0]

S4 ($^1A'$) [21.3]

S1 ($^1A'$) [0.0]

S2 ($^1A'$) [5.0]

Fig. 1 B3LYP/aug-cc-pVTZ–optimized geometries (bond lengths in pm; bond angles in degrees) of the seven lowest [H, Si, N, C, S] isomers in the $\tilde{X}^1A'$ electronic state. All energies [in kJ/mol] are relative to the lowest energy isomer (S1)

In order to check if the B3LYP calculations were giving the correct ordering of the seven lowest isomers, further calculations were carried out using different levels of theory. Higher level calculations were carried out at the MP2, QCISD and QCISD(T) levels of theory (using the aug-cc-pVTZ basis set) as implemented in the G03 package. For each calculation, the geometries were re-optimized and where possible the vibrational frequencies evaluated. In the case of the QCISD(T) calculations, the geometry was re-optimized at the QCISD level of theory and a single-point calculation at this geometry was carried out. Table 1 shows the relative energy differences between the lowest seven isomers found at each level of theory. For each method, the HSi(S)CN isomer is predicted to be the lowest in energy. For isomer S2, the QCISD calculations agree well with the B3LYP results; however, the MP2 calculations predict a difference of 24.7 kJ/mol, which is over three times that found using the other methods. Again for isomers S3 and S4, the B3LYP results agree well with the QCISD result. The MP2 results predict higher energies for both isomers; in particular, the *trans*-HSSiNC isomer which is predicted to be 53.1 kJ/mol higher in energy and is higher in energy than the isomer S5. The QCISD result for next two highest isomers, S5 and S6, agrees well with the B3LYP results, while the MP2 method again estimates much higher energies. The largest discrepancy is seen for the HSiNCS isomer. In this case, the B3LYP result of 43.9 kJ/mol is significantly lower than that predicted by the MP2 and QCISD methods which estimate an energy of ~79.5 kJ/mol. The QCISD(T) energies match those of QCISD except for the ordering of isomers S4 and S5.

The G3B3 and G3MP2 multilevel methods were carried out on the lowest seven isomers (in the $\tilde{X}^1A'$ electronic state) in order to determine more accurate relative energies. As can be seen from Table 1, the G3MP2 results agree well with the QCISD results and both methods show that isomer S1, as seen in Fig. 1, is the lowest lying isomer. For HSiNCS, the G3MP2 method again agrees well with the QCISD result and shows that the relative energy of HSiNCS is significantly higher than that predicted using B3LYP, which may indicate that the species may not be easily detected, unlike HSiNCO which had a relative energy of only ~56.5 kJ/mol and has been detected using laser-induced fluorescence [2]. The G3B3 results match those from the G3MP2 calculation, except in the ordering of isomers S4 and S5.

Table 1 Energies of the seven lowest [H, Si, N, C, S] isomers (in kJ/mol), relative to isomer 1 (as in Fig. 1)

Isomer	B3LYP	MP2	QCISD[a]	QCISD(T)[a]	G3B3[b]	G3MP2[b]
HSi(S)CN	0.0	0.0	0.0	0.0	0.0	0.0
HSi(S)NC	5.0	24.7	5.9	9.6	10.5	6.3
trans-HSSiCN	18.0	32.2	18.8	20.1	25.9	25.1
trans-HSSiNC	21.3	53.1	23.4	28.0	35.1	31.0
cis-HSSiCN	25.5	41.0	25.9	27.6	34.3	33.9
cis-HSSiNC	28.0	60.7	30.1	34.7	42.7	38.9
HSiNCS	43.9	81.6	76.6	74.0	69.0	70.7

All energies are ZPE corrected

[a] ZPE taken from MP2 calculation

[b] G3(E_0), $E_0 = E_{elec} + \mathrm{ZPE}$

Ding et al. [15] carried out an analysis of the isomers of [H, C_2, N, S] at the MP2/cc-pVDZ level of theory. The ordering of the [H, Si, N, C, S] isomers is similar to that of the carbon based isomers [H, C_2, N, S] with HC(S)CN (0.0 kJ/mol), HC(S)NC (98.3), *cis*-HSCCN (192.9), *trans*-HSCCN (191.6), *cis*-HCSCN (252.7) and *trans*-HCSNC (259.0). Interestingly, they failed to calculate the energy of the HCNCS isomer as well as a number of cyclic species. Earlier work by Flammang et al. [16] using the MP2/6-31G(d) level of theory, gave a slightly different ordering of the [H, C_2, N, S] isomers with the HC(S)CN isomer being the lowest, the next highest isomers were HNCCS (133.0 kJ/mol), *cyclic*-CHNCS (134.7), *trans*-HSCCN (157.7), HNCCS (194.5) and HCNCS (197.9).

3.1 HSi(S)CN/HSi(S)NC

The two lowest isomers energetically are HSi(S)CN and HSi(S)NC, which are analogous to thioformyl cyanide and thioformyl isocyanide. For both isomers, the Si–H bond length is 147 pm, which is similar to that observed for H_3SiNCS [17–19]. The Si–S bond length is predicted to be ~194 pm, which is similar to the 192.9 pm bond length observed in the diatomic SiS [20]. The H–Si–C/N angle of ~106° with the S–Si–C/N angle of 124.5° indicates that some sp^2 hybridisation is occurring on Si resulting in the ~120° angles. The dipole moments (μ_x/μ_y) at the B3LYP/aug-cc-pVTZ level of theory in the ground electronic state for HSi(S)CN and HSi(S)NC are -0.52/2.51 D and -0.15/2.29 D, respectively, and are sufficiently high that these species should be observed using standard microwave spectroscopy techniques. Table 2 shows the vibrational frequencies and rotational constants for these species at the B3LYP/aug-cc-pVTZ level of theory.

For HSi(S)CN, a natural bond orbital analysis (NBOA) shows the bonding contributions from Si for Si–H, Si–C and Si–S bonds involves some hybridisation $sp^{2.01}$ (66%, % *p*-character), $sp^{2.64}$ (72%) and $sp^{1.50}$ (60%), respectively, which explains the slightly larger H–Si–C and S–Si–C angles seen over the other isomers studied and is in line with typical sp^2 hybridisation angles. For HSi(S)NC the bonding is very similar to that seen for HSi(S)CN. The NBOA predicts no substantial delocalisations in either molecule.

3.2 Excited states

Calculations on the excited states of these species have been carried out with the aim of trying to detect these species

Table 2 Harmonic frequencies (in cm^{-1}) [Intensities (in km/mole)] and equilibrium rotational constants (in GHz) of the seven lowest [H Si, N, C, S] isomers in the $\tilde{X}^1A'$ state at the B3LYP/aug-cc-pVTZ level of theory

Species	Vibrational frequencies (intensities)	Rotational constants (A, B, C)
HSi(S)CN	134.4(11), 239.5(4), 357.6(1), 500.0(8), 569.8(49), 746.3(30), 852.7(132), 2272.6(46), 2290.7(39)	19.85253, 2.24140, 2.01401
HSi(S)NC	126.7(7), 174.7(1), 303.8(7), 504.8(11), 617.0(52), 777.7(62), 866.6(187), 2129.4(485), 2287.7(43)	21.46943, 2.43029, 2.18316
trans-HSSiCN	124.7(3), 214.4(1), 351.7(2), 473.8(6), 513.8(65), 548.3(84), 802.9(13), 2254.8(29), 2658.0(2)	10.62364, 2.74731, 2.18283
cis-HSSiCN	126.9(8), 212.3(15), 369.4(0), 417.1(17), 496.8(64), 543.4(88), 711.5(7), 2251.2(25), 2663.2(3)	10.57728, 2.69451, 2.14746
trans-HSSiNC	126.8(2), 164.1(0), 296.0(2), 431.5(5), 502.6(77), 610.5(140), 781.1(17), 2106.4(407), 2665.0(3)	11.91714, 2.86431, 2.30927
cis-HSSiNC	133.0(6), 160.2(6), 309.7(2), 386.2(19), 489.4(88), 590.6(122), 695.8(17), 2102.5(386), 2665.9(3)	12.02699, 2.79524, 2.26810
HSiNCS	102.7(1), 127.2(1), 462.1(41), 503.1(56), 519.7(1), 858.8(117), 1019.2(5), 2001.3(530), 2069.7(1360)	170.49781, 1.60324, 1.58830

Harmonic frequencies (cm^{-1}) = unscaled frequencies

using laser-induced fluorescence (LIF) spectroscopy. Our group has already successfully carried out spectroscopic measurements on HSiNC and HSiNCO in their $\tilde{A}^1A''$ excited state, and it is hoped that similar work will be carried out on some of the isomers outlined in this work [2, 3].

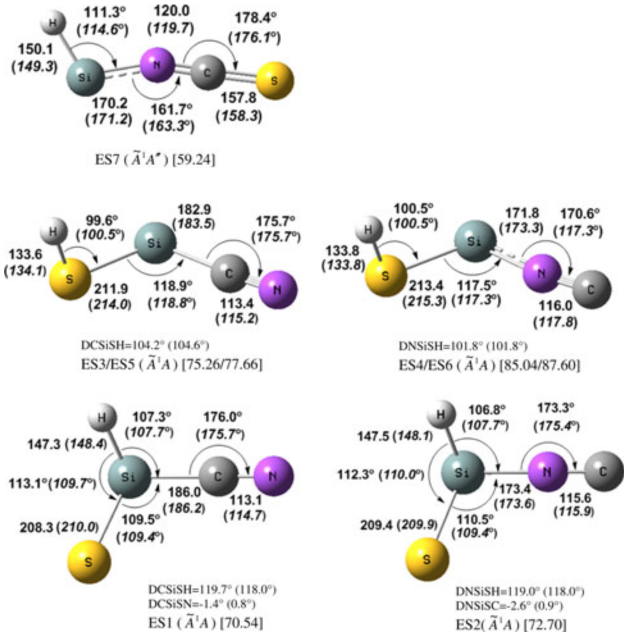

Fig. 2 CIS/aug-cc-pVTZ (SAC-CI/aug-cc-pVDZ)–optimized geometries of the $\tilde{A}^1A$ excited state of the six lowest [H, Si, N, C, S] isomers (bond lengths in pm; bond angles in degrees). All energies [in kJ/mol] are taken from SAC-CI calculations (not ZPEC) and are relative to their corresponding $^1A'$ isomers as in Fig. 1. For HSiNCS, the B3LYP/aug-cc-pVTZ(SAC-CI/aug-cc-pVDZ)–optimized geometry for the $\tilde{A}^1A''$ excited state is given

Excited state calculations on the planar $\tilde{A}^1A''$state for HSi(S)CN and HSi(S)NC indicated both to be a transition state. Both of these isomers are the Si/S analogues of formyl cyanide; work on formyl cyanide has shown that the first singlet excited state ($\tilde{A}^1A''$) results in the hydrogen atom bending substantially out of the molecular plane (~25.0°), but the associated potential function is flat and there is a low barrier to planarity (the inertial defect is $\Delta = 0.67$ amu Å^2) [21]. With this in mind calculations were carried out using the CIS and SAC-CI methods to investigate the structure of a non-planar excited state. The CIS/aug-cc-pVTZ and SACCI/aug-cc-pVDZ structures for the HSi(S)CN and HSi(S)NC excited state are shown in Fig. 2 (labelled ES1 and ES2, respectively). Upon electronic excitation [of the n(Si) → π^* type], both isomers are expected to undergo a large extension of the Si=S bond and a deformation of the planar structure as seen in analogous systems, such as formaldehyde and formyl fluoride [22, 23]. It can be seen from Fig. 2 that the Si=S bond does increase significantly (~20 pm) on excitation, which will result in the electronic spectrum having a long progression in the Si=S stretching mode. Other major changes in the geometry on excitation are the S–Si–H and S–Si–N/C angles decreasing to ~109°, which is in line with the change from sp^2 hybridisation on the Si to sp^3 hybridisation. For both species, the out-of-plane (OOP) angle between the SiS axis and the HSiC/N plane is ~60°. The resulting inertial defect for the two isomers in their excited state is calculated to be −2.46 amu Å^2 and −2.52 amu Å^2, respectively, clearly indicating that the excited state is non-planar. The potential function of the hydrogen atom bending out of the molecular plane for both isomers has been investigated and analysed using the double-minimum function used by Coon et al. (the details of this analysis can be found in the supplementary data) [24, 25]. The lowest lying triplet states for each isomer have also been looked at and in all cases they were found to be higher in energy (the details on the triplet states of the lowest seven isomers can be found in the supplementary data).

For both HSi(S)CN and HSi(S)NC, the structures of the ground and excited states were optimized using SAC-CI employing an aug-cc-pVDZ basis set. The calculations were carried out using singles and doubles linked excitations operators with 'level three' accuracy. A single-point calculation was then carried out on the optimized structure using the cc-pVTZ basis set. The SAC-CI calculations give the transition frequencies (not ZPE corrected) to the non-planar structure ($\tilde{A}^1A$) as 24,673 cm^{-1} and 26,327 cm^{-1}, for HSi(S)CN and HSi(S)NC, respectively.

3.3 HS-SiCN/HS-SiNC

As can be seen from Fig. 1, the geometry of these thiols show an S–H bond length (134.8 pm) which is similar to that observed in other thiols [26]. The average Si–S bond length is 215 pm, which is slightly smaller than the covalent radii sum (221 pm) and is similar to that seen in other silicon based thiols [27, 28]. The two most interesting structural aspects of these species are the S–Si–C/N and Si–S–H angles. The S–Si–C/N angle is small, ~95° and is similar to the H–Si-X angle found in HSiNC/CN (~95°), while the Si–S–H angle is inline with that observed for other alkylsilanthiols (~100°) and is 20° smaller than the OH analogues [28, 29]. In going from the *trans* to *cis* form, the H–S–Si angle increases by ~6°, which is probably result of repulsion effects. This is also reflected in the Si–S bond length which increases in going from the *trans* to the *cis* form.

Table 2 shows the vibrational frequencies at the B3LYP/aug-cc-pVTZ level of theory for *cis*/*trans* HS–SiCN and *cis*/*trans* HS-SiNC. At the B3LYP/aug-cc-pVTZ level of theory the dipole moments (μ_x/μ_y) of *cis* and *trans* HS-SiCN are −2.35/0.91 D and −3.48/2.06 D, respectively, while for *cis/trans* HS-SiNC they are, −1.91/0.57 D and −3.04/1.66 D, respectively. Again, the dipole moments of these species are large enough that they should be easily detected using microwave spectroscopic techniques.

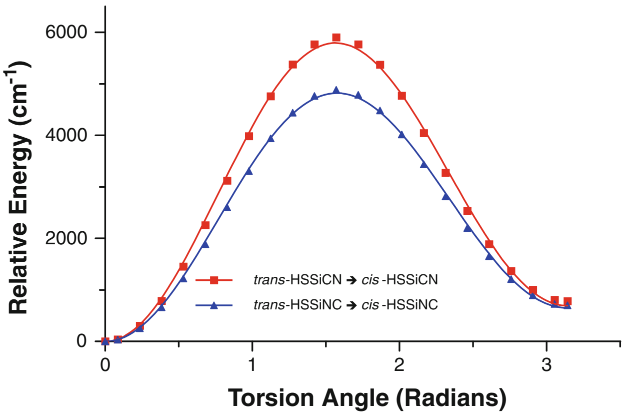

Fig. 3 *trans* to *cis* isomerisation of HSSiCN (*filled square*) and HSSiNC (*filled triangle*)

3.4 Isomerisation

For the *cis* and *trans* forms of HS-SiCN and HS-SiNC, calculations were performed on both species in order to determine the potential of rotation of the hydrogen about the sulphur atom. Figure 3 shows the isomerisation potential for both HS-SiCN and HS-SiNC. The potentials were generated by changing the HSSiC/HSSiN dihedral angle, while relaxing the rest of the structure at the B3LYP/aug-cc-pVTZ level of theory. A total of 20 points were calculated for each species. From Fig. 3, it can be seen that the potential has a double minimum at 0 and 180°, corresponding to the *trans* and *cis* forms, respectively, where θ is the dihedral angle between H–S-Si–C/N. In both cases the *cis* form is higher in energy by ~1.25 kJ/mol, which is similar to that found for formic, thiolformic, thionformic and dithioformic acids but opposite to that found for HO-SiCN/NC. The potentials have been fitted using the function of Torro-Labbe et al. [30]:

$$V(\theta) = \frac{1}{2}\Delta V^\circ(1-\cos\theta) + \frac{1}{4}(k_t+k_c)\left(1-\cos^2\theta\right) + \frac{1}{4}(k_t-k_c-\Delta V^\circ)\left(1-\cos^2\theta\right)\cos\theta. \tag{1}$$

The data from the fits are shown in Table 3 and are compared against the results found for HO-SiCN, HO-SiNC, thiolformic, thionformic and dithioformic acids using the same method [1, 30]. It can be seen that HS-SiCN and HS-SiNC have similar, although slightly higher, barrier heights than thionformic and dithioformic acids. The values of k_t and k_c are similar to those of thionformic and dithioformic acids with the k_t force constant larger than k_c. These force constants indicate that for the *cis* form there is some repulsive interaction which destabilizes the system; the opposite is seen for HO-SiCN/NC [1]. The parameters α and $\Delta V^\ddagger$ are the angle in which the potential is at a maximum and the barrier height, respectively. For HS-SiCN $\alpha = 89.68^\circ$ and $\Delta V^\ddagger = 5{,}791.32$ cm^{-1}, while for HS-SiNC $\alpha = 90.19^\circ$ and $\Delta V^\ddagger = 4{,}819.65$ cm^{-1}.

NBOA on HS-SiCN shows that the bonding between Si–S and Si–C is mainly *p* in character (>85%) for both the *cis* and *trans* species. The almost pure *p*-character of these MOs explains the relatively small S–Si–C angle seen in both isomers. As expected the NBOA for *cis*/*trans* HS-SiNC is very similar to that of *cis*/*trans* HS-SiCN.

3.5 Excited state

Calculations have also been carried out on the first $^1A''$state of each species. As found for HSi(S)CN and HSi(S)NC

Table 3 Parameters for HS-SiNC and HS-SiCN from the second potential function (Eq. 1) where k_c and k_t (force constants) in kcal mol^{-1} rad^{-2}, V_1,V_2,V_3, ΔV^0 and $\Delta V^{\ddagger}$ in cm^{-1} and α_0 in degrees

Parameters	HS-SiCN	HS-SiNC	HO-SiCN[a]	HO-SiNC[a]	HS(O)CH[b]	HO(S)CH[b]	HS(S)CH[b]
k_c	27.80	23.08	18.63	15.93	15.41	16.63	17.17
k_t	34.46	28.31	15.23	13.92	20.40	30.79	25.45
V_1	−245.04	−251.92	−278.17	−278.59	–	–	–
V_2	−2722.00	−2247.00	−1480.45	−1304.99	–	–	–
V_3	−102.11	−73.67	97.08	69.91	–	–	–
ΔV^0	694.3	651.2	362.2	417.4	495.6	2236.7	611.0
α_0	89.68	90.19	95.42	95.29	92.0	93.0	92.0
$\Delta V^{\ddagger}$	5791.32	4819.65	3169.04	2841.28	3379.7	5276.9	4037.0

[a] Ref. [1]

[b] Ref. [30]

analysis of the excited $\tilde{A}^1A''$ state for these isomers indicated them to be transition states. As a result of this CIS and SAC-CI calculations were carried out on the $\tilde{A}^1A$ electronic state for each isomer. The CIS/aug-cc-pVTZ and SACCI/aug-cc-pVDZ structures for the $\tilde{A}^1A$ excited state HS-SiCN and HS-SiNC are shown in Fig. 2 (ES3/ES5 and ES4/ES6). Each isomer has one common non-planar excited state structure. On excitation there is a significant increase in the S–Si–C/N angle (~20°) which is probably a result of density being shifted to an in-plane *p* orbital on Si resulting in further sp^2 hybridisation. Another significant change is in the Si–C/N bond length which decreases by ~5 pm on excitation. The largest change is with the H atom, which has moved substantially out of the molecular plane and now has an OOP angle (with respect to the S–Si–C/N plane from the planar *cis* form) of 104 and 102° (CIS/aug-cc-pVTZ geometry), for HS-SiCN and HS-SiNC, respectively. The reason for this large OOP angle is unclear, although it is probably a result of sp^3 hybridisation on the sulphur atom. The inertial defect for HS-SiCN and HS-SiNC is −3.18 and −3.23 amu Å^2, respectively, which clearly indicates a non-planar structure. The SAC-CI calculations give the transition frequency to the non-planar excited state (not ZPE corrected) as *cis*/*trans* HS-SiCN 26326/27162 cm^{-1}, while for *cis*/*trans* HS-SiNC the transition frequencies are 29744/30640 cm^{-1}, respectively.

3.6 HSiNCS

The ground electronic state structure of HSiNCS is analogous to HSiCN, HSiNC and HSiNCO with the H–Si-X angle being around 95°. The small H–Si-X angle is also seen for the analogous halogen species HSiX (X = F, Cl, Br, I) with the H–Si-X angle going from 96.9, 96.9, 102.9, and 102.7°, respectively [31–35]. The Si–H bond length of 152.7 pm is almost identical to that found for HSiNC (152.6 pm); however, it is ~4 pm longer than the Si–H bond in H_3SiNCS [36]. The question of linearity or non-linearity of the N=C=S group has, like the N=C=O group, been of much interest for several decades [37]. As found for the N=C=O group, NBOA proposes three resonance structures with the N=C=S being the most probable, while $^{+}N{\equiv}C{-}S^{-}$ and $^{-}N{-}C{\equiv}\ S^{+}$ being the other minor forms. It is highly likely that the N=C=S group is in fact non-linear based on the proposed resonance structures. However, in most of the early microwave spectroscopy and electron diffraction studies, the N=C=S group was assumed to be linear. Only in a few cases has the N=C=S angle actually been determined experimentally. For the microwave spectroscopy studies, it has been found that fixing the NCS group to being linear typically gives a poor fit to the observed frequencies. However, fits have been improved by using increasingly complex Hamiltonians, incorporating bending and rotational terms [17, 18]. By comparison, ab initio studies on species containing the NCS group have typically found the N=C=S angle to be only slightly less than 180°, with the average angle being between 175 and 179.9° [38].

Vibrational frequencies and rotational constants for HSiNCS in its ground electronic state were also calculated and are given in Table 2. The dipole moments (μ_x/μ_y) at the B3LYP/aug-cc-pVTZ level of theory were calculated to be 0.32/1.26 D. The dipole moments for HSiNCS are less than the previous isomers studied; however, they should be still large enough for detection using standard microwave spectroscopy techniques. The NBOA analysis shows the bonding between Si–H and Si–N is 85.8 and 98.6% *p* in character on the Si, which is similar to that seen in the HS-SiCN/NC isomers. The high *p*-character explains the small predicted H–Si–N bond angle of 96°.

3.7 Excited state

In 2009, Dover and Evans performed laser-induced fluorescence (LIF) experiments on the $\tilde{A}^1A''$ electronic state of HSiNCO [2]. It is thought that the same state should be observable for HSiNCS using a suitable precursor. Table 4

Table 4 Bond distances (pm), bond angles (degrees), dipole moments (Debye) and transition energies (cm^{-1}) for the $\tilde{A}^1A''$state of HSiNCS

Parameter	B3LYP	MP2	MC-SCF	SAC-CI[a]	Exp
r(H–Si)	150.1	148.7	154.2	149.3	
r(Si–N)	170.2	170.9	170.3	171.2	
r(N–C)	120.0	119.1	119.2	119.7	
r(C–S)	157.7	157.5	159.0	158.3	
∠(H–Si–N)	111.2	115.8	113.2	114.6	
∠(Si–N–C)	161.7	166.2	160.2	163.3	
∠(N–C–S)	178.4	178.9	178.4	176.1	
μ_x	0.085	0.532	–	–	
μ_y	−1.396	1.718	–	–	
T_0	13,578	16,163	20,724	20,720[b]	
HSiCN			20,567[c]	17,165	–
HSiNC			21,938[c]	19,765	19,950[d]
HSiNCO	14,485[e]	16,342[e]	21,700[e]	20,809[b]	20,346[f]
HSiF				23,693	23,260 [g]
HSiCl				21,111	20,718 [h]

[a] SAC-CI ZPE taken from B3LYP/aug-cc-pVTZ calculation

[b] cc-pVTZ basis set was used

[c] Ref. [43]

[d] Ref. [3]

[e] Ref. [1]

[f] Ref. [2]

[g] Ref. [33]

[h] Ref. [35]

shows calculations carried out on the $\tilde{A}^1A''$ state of HSiNCS. It shows that on excitation the H–Si–N angle increases significantly. This increase is due to electron density being transferred from a lone-pair on the Si atom to an out-of-plane *p* orbital on the Si atom. This transfer of electron density results in an increase in hybridisation (i.e. sp^2) on the Si atom and therefore opens up the H–Si–N bond angle. The H–Si–N angle increases from ~94° to ~115°, an increase which is similar to that seen in HSiNCO [1, 2]. Comparable increases are seen for the halogen species, HSiX ($X = $ F, Cl, Br, I), where on excitation the H–Si-X angles opens up to 115.0, 118.1, 116.6, and 116.2°, respectively [31–35].

Analysis of the $\tilde{A}^1A''$–$\tilde{X}^1A'$ transition energy was carried out using the SAC-CI method as implemented in G03 using a cc-pVTZ basis set. The results from the SAC-CI calculations are given in Table 4. For comparison the HSiF, HSiCl, HSiNC, HSiCN and HSiNCO transition energies were also evaluated at the same level of theory but using the aug-cc-pVTZ basis. As can be seen in Table 4, the SAC-CI calculations are in excellent agreement with the experimental results for HSiF, HSiCl, HSiNC and HSiNCO; therefore, the predicted transition frequency of 20,400 cm^{-1} for HSiNCS, even with the smaller cc-pVTZ basis set, which was used because of computer limitations, should be within ~600 cm^{-1} of the true value.

Table 5 Enthalpy of formation at 0 and 298 K of the seven lowest [H, Si, N, C, S] isomers (in kJ/mol)

Isomer	$\Delta_f H^0$[G3MP2]	
	0 K	298 K
HSi(S)CN	192.5	206.3
HSi(S)NC	199.2	213.0
trans-HSSiCN	217.6	231.8
trans-HSSiNC	223.4	238.1
cis-HSSiCN	226.3	241.0
cis-HSSiNC	231.8	246.4
HSiNCS	263.2	277.4

3.8 Enthalpy of formation

In order to get some understanding of how the chemical structures of the isomers relate to their reactivity, the enthalpies of formation of the lowest seven isomers were evaluated. Table 5 shows the enthalpy of formation at 0 and 298 K of the seven lowest [H, Si, N, C, S] isomers using the G3MP2 multilevel method. The enthalpies of formation at 298 K for the seven lowest [H, Si, N, C, S] isomers range between 251 and 335 kJ/mol. The enthalpies were calculated using the method of Curtiss et al. [39] where the theoretical enthalpies were calculated by subtracting the calculated atomization energies from the known enthalpies of formation of the isolated atoms. To calculate the enthalpy of formation at 0 K, Eq. [2] was employed:

$$\Delta H^{\circ}_{f,0}(M) = E(M) + ZPE(M) - \sum_{z}^{\text{atoms}} E(X_z) + \sum_{z}^{\text{atoms}} \Delta H^{\circ}_{f,0}(X_z) \quad (2)$$

while for the enthalpy of formation at 298 K Eq. 3 was used:

$$\Delta H^{\circ}_{f,298}(M) = E(M) + ZPE(M) + [H_{298}(M) - H_0(M)] - \sum_{z}^{atoms} \{E(X_z) + [H_{298}(X_z) - H_0(X_z)]\} + \sum_{z}^{atoms} \Delta H^{\circ}_{f,298}(X_z) \quad (3)$$

In Eq. 3, $H_{298}(M)$ and $H_0(M)$ are taken from the theoretical calculations, while the values of H_{298}-H_0 for the atoms were taken from the JANAF tables, as with the values for $\Delta H^{\circ}_{f,0}$ and $\Delta H^{\circ}_{f,298}$ for the atoms [40]. A test calculation on HNCS was carried out using the G3MP2 multilevel method and $\Delta H^{\circ}_{f,0}$ and $\Delta H^{\circ}_{f,298}$ where estimated to be 127 and 136 kJ/mol, respectively, which are in good agreement with the experimental values of $\Delta H^{\circ}_{f,0} \geq 129.7 \pm 2.9$ and $\Delta H^{\circ}_{f,298} \geq 127.2 \pm 2.9$ kJ/mol [41].

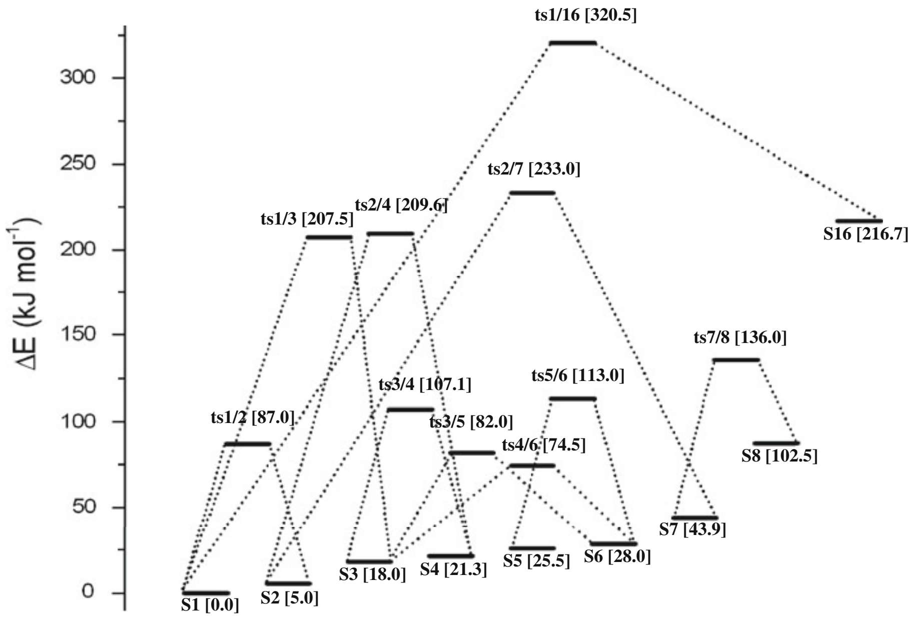

Fig. 4 Schematic of the potential energy surface of the seven lowest isomers of [H, Si, N, C, S] at the B3LYP/aug-cc-pVTZ level of theory

It is very difficult to compare these results with previous work as there is no thermodynamic data on species containing H, Si, C, N and S. If we compare the enthalpies of formation against similar silicon and carbon-containing transient species then we see that the generation and detection of the seven lowest [H, Si, N, C, S] isomers is, from a thermodynamic standpoint, possible. For instance, the enthalpy of formation of HNCS (298 K) has been estimated to be 129.7 kJ/mol, while work on NCS has estimated that $\Delta H^{\circ}_{f,298} \sim 320.1\,\mathrm{kJ/mol}$, which is similar to the species studied in this paper [41]. If we compare the results against some recently studied short-lived silicon-containing species such as, SiCH ($\Delta H^{\circ}_{f}(298\,\mathrm{K}) = 515\,\mathrm{kJ/mol}$), $H_2Si{=}CH_2$ ($\Delta H^{\circ}_{f}(298\,\mathrm{K}) = 179.9\,\mathrm{kJ/mol}$), SiC ($\Delta H^{\circ}_{f}(298\,\mathrm{K}) = 747.3$ kJ/mol), SiC_2 ($\Delta H^{\circ}_{f}(298\,\mathrm{K}) = 623.8\,\mathrm{kJ/mol}$), SiCN($\Delta H^{\circ}_{f}$ $(298\,\mathrm{K}) = 433.4\,\mathrm{kJ/mol}$), SiNC ($\Delta H^{\circ}_{f}(298\,\mathrm{K}) = 444.7$ kJ/mol), HSiCN ($\Delta H^{\circ}_{f}(298\,\mathrm{K}) = 360.1\,\mathrm{kJ/mol}$), HSiNC ($\Delta H^{\circ}_{f}(298\,\mathrm{K}) = 365.7\,\mathrm{kJ/mol}$) and $SiCH_2$ ($\Delta H^{\circ}_{f}(298\,\mathrm{K}) =$ $312.1\,\mathrm{kJ/mol}$) [42–44], it shows, again, that the species examined in this work should be observable in the laboratory and possibly in the stellar and interstellar medium.

Overall, if the correct generation technique is employed (i.e. photolysis, pyrolysis, laser ablation or electric discharge) in conjunction with the right pre-cursor then the spectroscopic detection of some of the proposed [H, Si, N, C, S] isomers is highly feasible with the best method of detection being most probably microwave spectroscopy.

3.9 Transition states

Figure 4 shows some of the various isomerisation processes between the seven lowest isomers (see the supplementary data for the structures of the transition states). For **S1** and **S2** the barrier of the CN → NC interconversion *via* the **ts1/2** transition state is very similar to that seen in HSiCN/NC with **S1** → **S2** (87.0 kJ/mol) and **S2** → **S1** (82.0 kJ/mol) [45]. The conversion of **S1** to **S3** via **ts1/3** and **S2** to **S4** via **ts2/4** are energetically very similar to each other. The conversion of **S3** to **S4** via **ts3/4** has a similar barrier to that seen for the interconversion between **S1** and **S2**. The conversion of **S3** to **S5** and **S4** to **S6** has been discussed in detail in a previous section (i.e. isomerisation); the **S4** to **S6** conversion via **ts4/6** is more favourable than the **S3** to **S5** conversion via **ts3/5**. **S5** can undergo conversion to **S6** via **ts5/6** with a barrier similar to that seen for **S3** → **S4** and **S1** → **S2**. **S2** can undergo conversion to **S7** via **ts2/7**. The barrier for **S2** → **S7** is 228.0 kJ/mol, while for **S7** → **S2** it is 189.1 kJ/mol showing that the high-energy conversion between the two is not favourable. Another high-energy conversion process can occur between **S1** and **S16**, which is HSiSCN, via the **ts1/16** transition state. The barrier for this interconversion is 320.5 kJ/mol from **S1** to **S16** and 103.8 kJ/mol from **S16** to **S1.** Finally, the conversion between **S7** and **S8** (HSiSCN) shows the barrier from **S7** → **S8** (92 kJ/mol) is higher than the barrier going from **S8** → **S7** (33.5 kJ/mol).

4 Conclusion

In this work, we have looked at a number of [H, Si, N, C, S] isomers in different electronic states. This is the first ever study on these species. It has been found that the HSi(S)CN isomer is the lowest energy isomer with the seven lowest isomers being within 83.7 kJ/mol of each other. One of the main reasons for this paper was to calculate constants to aid in the detection of these species spectroscopically. To do this, we have calculated vibrational frequencies and equilibrium rotational constants of the seven lowest isomers in their ground electronic state. For each of these isomers, we have also determined the structure and transition energy of the first singlet electronic state. We have also determined the enthalpy of formation of the seven lowest isomers using the G3MP2 multilevel method and have found that, for the most part, the species are relatively thermodynamically stable with the enthalpies of formation comparable to those of other silicon-containing species that have been detected spectroscopically e.g. SiC_2 and $SiCH_2$. Lastly, we have looked at the isomerisation processes between the lowest lying isomers and determined transition states linking them. Overall, it is thought the isomers investigated in this work should be observable in their ground electronic state using spectroscopic techniques, in particular, microwave spectroscopy. Given also that these species are fairly thermodynamically stable, it is reasonable to assume that these species may also be present in the stellar and interstellar medium.

Acknowledgments SRTN would like to thank the Nuffield Foundation for a Nuffield Science Bursary.

References

1. Dover MR, Evans CJ (2007) J Phys Chem A 111:13148
2. Dover MR, Evans CJ, Western CM (2009) J Chem Phys 131, Artn 124302
3. Evans CJ, Dover MR (2009) J Phys Chem A 113:8533
4. Boyle RJ, Keady JJ, Jennings DE, Hirsch KL, Wiedemann GR (1994) Astrophys J 420:863
5. Frisch MJ, Trucks GW, Schlegel HB, Scuseria GE, Robb MA, Cheeseman JR, Montgomery JJA, Vreven T, Kudin KN, Burant JC, Millam JM, Iyengar SS, Tomasi J, Barone V, Mennucci B, Cossi M, Scalmani G, Rega N, Petersson GA, Nakatsuji H, Hada M, Ehara M, Toyota K, Fukuda R, Hasegawa J, Ishida M, Nakajima T, Honda Y, Kitao O, Nakai H, Klene M, Li X, Knox JE, Hratchian HP, Cross JB, Bakken V, Adamo C, Jaramillo J, Gomperts R, Stratmann RE, Yazyev O, Austin AJ, Cammi R, Pomelli C, Ochterski JW, Ayala PY, Morokuma K, Voth GA, Salvador P, Dannenberg JJ, Zakrzewski VG, Dapprich S, Daniels AD, Strain MC, Farkas O, Malick DK, Rabuck AD, Raghavachari K, Foresman JB, Ortiz JV, Cui Q, Baboul AG, Clifford S, Cioslowski J, Stefanov BB, Liu G, Liashenko A, Piskorz P, Komaromi I, Martin RL, Fox DJ, Keith T, Al-Laham MA, Peng CY, Nanayakkara A, Challacombe M, Gill PMW, Johnson B, Chen W, Wong MW, Gonzalez C, Pople JA (2004) Gaussian 03 revision E.01. Gaussian Inc., Wallington CT
6. Dunning TH (1989) J Chem Phys 90:1007
7. Woon DE, Dunning TH (1993) J Chem Phys 98:1358
8. Møller C, Plesset MS (1934) Phys Rev 46:618
9. Becke AD (1993) J Chem Phys 98:5648
10. Werner HJ, Knowles PJ, Lindh R, Manby FR, Schütz M, Celani P, Korona T, Rauhut G, Amos RD, Bernhardsson A, Berning A, Cooper DL, Deegan MJO, Dobbyn AJ, Eckert F, Hampel C, Hetzer G, Lloyd AW, McNicholas SJ, Meyer W, Mura ME, Nicklaß A, Palmieri P, Pitzer R, Schumann U, Stoll H, Stone AJ, Tarroni R, Thorsteinsson T (2002) MOLPRO version (2002.1) Cardiff, UK
11. Nakatsuji H (1979) Chem Phys Lett 67:334
12. Reed AE, Curtiss LA, Weinhold F (1988) Chem Rev 88:899
13. Schaftenaar G, Noordik JH (2000) J Comput Aided Mol Des 14:123
14. Dennington R II, Keith T, Millam J, Eppinnett K, Hovell WL, Gilliland R (2003) GaussView, Version 3.09. Semichem, Shawnee Mission, KS
15. Ding WH, Fang WH, Liu RZ (2003) THEOCHEM 623:327
16. Flammang R, Landu D, Laurent S, Barbieux-Flammang M, Kappe CO, Wong MW, Wentrup C (1994) J Am Chem Soc 116:2005
17. Dossel KF, Robiette AGZ (1977) Naturforsch A: Phys Sci 32:462
18. Dossel KF, Sutter DHZ (1977) Naturforsch A: Phys Sci 32:473
19. Duckett JA, Robiette AG, Gerry MCL (1981) J Mol Spectrosc 90:374
20. Muller HSP, McCarthy MC, Bizzocchi L, Gupta H, Esser S, Lichau H, Caris M, Lewen F, Hahn J, Esposti CD, Schlemmer S, Thaddeus P (2007) Phys Chem Chem Phys 9:1579
21. Clouthier DJ, Karolczak J, Rae J, Chan WT, Goddard JD, Judge RH (1992) J Chem Phys 97:1638
22. Clouthier DJ, Ramsay DA (1983) Annu Rev Phys Chem 34:31
23. Ding HB, Orr-Ewing AJ, Dixon RN (1999) Phys Chem Chem Phys 1:4181
24. Coon JB, Naugle NW, McKenzie RD (1966) J Mol Spectrosc 20:107
25. Jones VT, Coon JB (1969) J Mol Spectrosc 31:137
26. Csizmadia G (1974) General and theoretical aspects of the thiol group. In: Patai S (ed) The chemistry of the thiol group vol 1. Wiley, London
27. Sanderson RT (1983) J Am Chem Soc 105:2259
28. Herman A, Wojnowski W (1992) Struct Chem 3:239
29. Sanz ME, McCarthy MC, Thaddeus P (2002) Astrophys J 577:L71
30. Toro-Labbe A (1988) THEOCHEM 180:209
31. Billingsley J (1972) Can J Phys 50:531
32. Herzberg G, Verma RD (1964) Can J Phys 42:395
33. Dixon RN, Wright NG (1985) Chem Phys Lett 117:280
34. Harper WW, Clouthier DJ (1997) J Chem Phys 106:9461
35. Harper WW, Hostutler DA, Clouthier DJ (1997) J Chem Phys 106:4367
36. Glidewel CMSG, Robiette AG (1972) Chem Phys Lett 16:526
37. Hargittai I, Paul IC (1977) Structural chemistry of the cyanates and their thio derivatives. In: Patai S (ed) The chemistry of cyanates and their thio derivatives, vol 1. Wiley, Chichester, pp 69
38. Palmer MH, Nelson AD (2004) J Mol Struct 689:161
39. Curtiss LA, Raghavachari K, Redfern PC, Pople JA (1997) J Chem Phys 106:1063
40. Chase MW, Jr (1998) NIST-JANAF thermochemical tables, 4th edn. Monograph No. 9, 1963 pp, ISBN: 1-56396-831-2
41. Ruscic B, Berkowitz J (1994) J Chem Phys 101:7975
42. Ketvirtis AE, Bohme DK, Hopkinson AC (1995) J Phys Chem 99:16121
43. Flores JR (2005) Chem Phys 310:303
44. Flores JR, Perez-Juste I, Carballeira L (2005) Chem Phys 313:1
45. Wang Q, Ding YH, Sun CC (2006) Chem Phys 323:413